

# Microstructure change of duplex stainless steels after thermal aging and electron beam irradiation

Yuta Suzuki<sup>a</sup>, Naoyuki Hashimoto<sup>b,\*</sup>

<sup>a</sup> Graduate School of Engineering, Hokkaido University, Sapporo 060-8628, Japan

<sup>b</sup> Faculty of Engineering, Hokkaido University, N13W8, Kita-ku, Sapporo 060-8628, Japan



## ARTICLE INFO

### Keywords:

Spinodal decomposition  
Accelerated irradiation  
Thermal aging

## ABSTRACT

Duplex stainless steel has been used as a structural material for light water reactors. It is well known that the thermal aging during operation causes spinodal decomposition to Cr-rich ( $\alpha'$ ) phase and Fe-rich ( $\alpha$ ) phase in the ferrite phase, resulting in embrittlement. In order to understand the mechanism of this phenomena and the effect of irradiation, a duplex model alloy (Fe-25Cr-10Ni-2.5Mo-1Mn) prepared by arc melting and thermally aged in the appropriate condition was subjected to accelerated irradiation by a multi-beam ultra-high voltage electron microscope and partially an ion accelerator in this study. Spinodal decomposition of Fe and Cr was confirmed in the model alloy aged at 450 °C. In addition, the electron beam irradiation to aged model alloy resulted in the decrease in the amplitude of spinodal decomposition. From this experiment, it was suggested that spinodal decomposition could be suppressed by accelerated irradiation.

## 1. Introduction

Duplex stainless steel has been used as a structural material for light water reactors due to its strength, irradiation resistance and corrosion resistance. Duplex stainless steel is consisted of ferrite phase and austenite phase. It is well known that thermal aging during operation causes spinodal decomposition to Cr-rich ( $\alpha'$ ) phase and Fe-rich ( $\alpha$ ) phase in the ferrite phase and G-phase ( $M_6Ni_{16}Si_6$ , M = Mn, Mo etc.) precipitation, resulting in embrittlement [1–5]. MD simulation for neutron-irradiated reactor pressure vessels indicated that the formation of displacement cascade would cause atomic mixing and this disordering could inhibit spinodal decomposition [6]. In addition, the neutron irradiation may also change the location of the phase fields in the phase diagram and effect on the decomposition process [7]. Miller et al. investigated a neutron-irradiated Fe-32Cr by using atom probe field ion microscopy [8], and reported the enhancement of spinodal decomposition. This result is consistent with the neutron irradiation significantly changing the location of the phase field in the phase diagram. Furthermore, it was reported that neutron-irradiated stainless-steel (90% austenite and 10%  $\delta$ -ferrite phases) showed spinodal decomposition in a manner similar to that resulting from thermal aging [9]. In order to clarify the mechanism of this complicated phenomena, it is necessary to carefully investigate the superimposition effect of neutron irradiation and thermal aging, however, it is difficult to perform neutron irradiation and thermal aging simultaneously. One solution would

be the simulated irradiation by electron beam and in-situ observation of microstructure change. Nakai and Kinoshita reported the e-irradiation-induced spinodal decomposition in alloys [10], but less in-situ observation studies in Fe-Cr system. In this study, a duplex model alloy was prepared and thermally-aged in some conditions, the electron irradiation was performed by using a multi-beam ultra-high voltage electron microscope in order to clarify the effect of defect flow on spinodal decomposition.

## 2. Experimental

Material used in this study was a duplex model alloy (Fe-25Cr-10Ni-2.5Mo-1Mn) arc-melted in Ar atmosphere. Table 1 shows the chemical composition of the model alloy. Si was detected by absorptiometry and Cr, Ni, Mn and Mo were detected by ICP emission spectroscopy. Fig. 1 shows a STEM-EDS mapping of the model alloy annealed at 700 °C for 1.5 h. In general, ferrite-forming elements (Cr and Mo) tend to dissolve in the ferrite phase and an austenite-forming element (Ni) does in the austenite phase. The model alloy was thermally aged at 450 °C for 480, 1000, and 3400 h in vacuum. The aging temperature was decided in order to successfully introduce spinodal decomposition in the model alloy. The aged model alloy was gently ground down to 0.15 mm in thick, and punched out to 3 mm $\phi$ . This disk was electro-polished by “–5% perchloric acid + acetic acid solution” at room temperature. TEM observation was performed to several samples using a

\* Corresponding author.

E-mail address: [hasimoto@eng.hokudai.ac.jp](mailto:hasimoto@eng.hokudai.ac.jp) (N. Hashimoto).

**Table 1**  
Chemical composition of the model alloy (wt%).

Cr	Ni	Mn	Mo	Si	Fe
24.87	10.07	0.87	2.51	0.01	Bal.

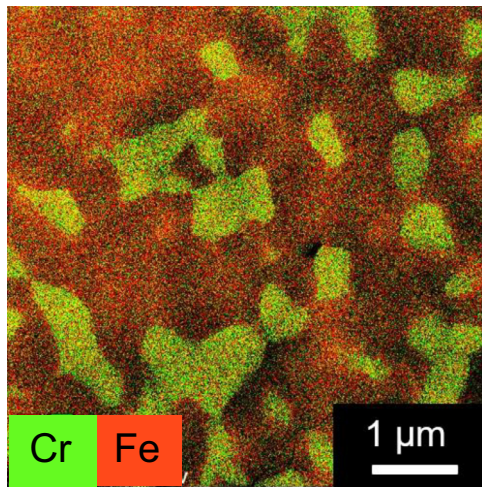


**Fig. 1.** STEM-EDS mapping of Fe (red) and Cr (green) in the model alloy annealed at 700 °C for 1.5 h. The red area indicates  $\gamma$ -phase (Fe-10 wt%Cr) and the green area does  $\alpha$ -phase (Fe-35 wt%Cr). (For interpretation of the references to colour in this figure legend, the reader is referred to the web version of this article.)

**Table 2**  
Electron-irradiation experiment condition.

Dose rate (dpa/s)	$1 \times 10^{-4}$ – $1 \times 10^{-3}$
Temperature (°C)	250–400
Dose (dpa)	0.1–10

conventional TEM (JEM-2010, JEOL) at accelerating voltage of 200 keV. STEM observation was performed using a Cs-corrected STEM (Titan) at accelerating voltage of 300 keV. In order to eliminate the contamination, Plasma Cleaning was performed prior to STEM observation. Electron irradiation experiment was performed using a multi-beam ultra-high electron microscope (JEM-ARM-1300, JEOL) operated at 1250 keV. The current density of electron beam was measured by Faraday cup inserted into the beam line. The electron beam flux on specimen surface can be controlled by changing beam size and calculated from the electron beam current density. The damage rate (dpa/s) of specimen was calculated from the beam flux and the displacement

per atom cross-section of elements. In addition, the electron irradiation temperature was controlled by the heating stage of specimen holder. The increase in temperature of the irradiated area would be at most several percent. The thickness of irradiated area was estimated by using the thickness fringes from the extinction distance of  $g$  vector. Table 2 shows the condition of electron irradiation experiment. After the electron irradiation experiment, the number density and size of dislocation loops were analyzed using conventional TEM.

### 3. Results

#### 3.1. Microstructural evolution in non-aged sample

Fig. 2 shows typical bright field images of ferrite phases in non-aged sample after electron-irradiation to 0.1 dpa and 1 dpa at 300 °C. The imaging condition was  $B \sim [001]$ ,  $g = 200$ , and  $s \sim 0$ . Fig. 3 shows the number density and the average diameter of dislocation loops in the electron-irradiated area. The number density and the average size of the irradiation-induced loops were increased as increasing irradiation dose. Fig. 4 shows typical bright field images of ferrite phases in non-aged sample after electron irradiation at 250, 300, 350, and 400 °C. The imaging condition was  $B \sim [001]$ ,  $g = 200$ , and  $s \sim 0$ . During electron irradiation, the number density and the average diameter of loops was decreased and increased as increasing irradiation temperature, respectively. Figs. 5 and 6 show the EDS mappings in ferrite phase irradiated to 10 dpa at 250 and 300 °C, respectively. The contrast of spinodal decomposition seemed not to be observed in this irradiation condition, but the enrichment of Fe at dislocation loop was observed instead.

#### 3.2. Microstructural evolution in aged sample

HR-TEM observation was performed to ferrite phase aged at 450 °C for 480 h and 1000 h, the contrast of spinodal decomposition was recognized in all the samples. The contrast of Fe and Cr became higher as increasing thermally aging time. On the other hand, G-phase was not clearly observed in both irradiated and aged model alloy probably due to a lack of Si for G-phase formation. Fig. 7 shows the EDS mapping and the bright field image of ferrite phase aged at 450 °C for 3400 h, and also the line analysis of solute concentration measured by STEM. TEM observation recognized a strong contrast in matrix, however there was no extra spot shown in diffraction pattern. This strong contrast could be due to spinodal decomposition by aging. The mean Cr concentration of the Fe-enriched regions in the ferrite during aging was evaluated by the decomposition fraction ( $\gamma$ ), which was obtained by Mossbauer spectroscopy [11]. The decomposition fraction ( $\gamma$ ) is given by  $\gamma = (C_t - C_0)/(C_\infty - C_0) \times 100$ , where  $C_0$  is the mean Cr concentration of the none-aged material,  $C_t$  is the mean Cr concentration of the Fe-enriched regions of the material aged for  $t$  hours, and  $C_\infty$  is the mean Cr

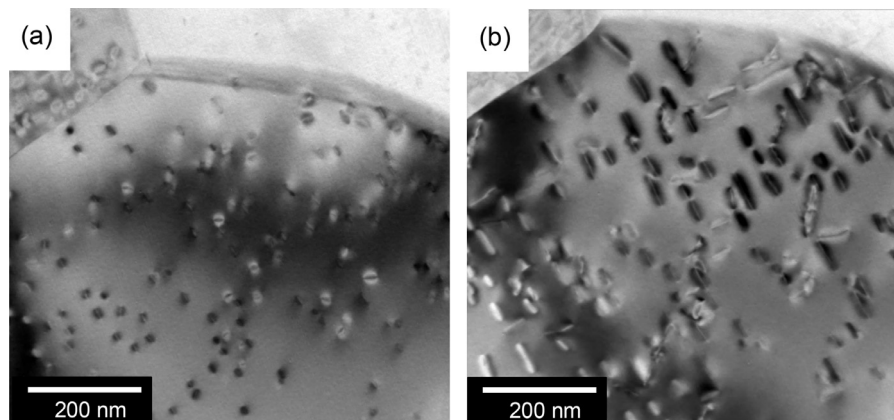


**Fig. 2.** Typical bright field images of ferrite phases in non-aged sample after electron irradiation to (a) 0.1 and (b) 1 dpa at 300 °C.

Download English Version:

<https://daneshyari.com/en/article/7987338>

Download Persian Version:

<https://daneshyari.com/article/7987338>

[Daneshyari.com](https://daneshyari.com)